Fifteenth USA/Europe Air Traffic Management Research and Development Seminar (ATM2023)

Designing a Framework of Integrated Aircraft Departure and Surface Traffic Operation via Queuing Network Models

Eri Itoh
The University of Tokyo, RCAST and Dept. Aeronautics and Astronautics
ENRI, Air Traffic Management Department
Tokyo, Japan
eriitoh@g.ecc.u-tokyo.ac.jp, eri@mpat.go.jp

Michael Schultz
Bundeswehr University Munich
Institute of Flight Systems
Munich, Germany
michael.schultz@unibw.de

***Abstract*—This study proposes model-based frameworks to design air traffic management systems, which enable us to control time-varying traffic inflow and outflow rates while balancing their capacities and demands. Furthermore, the proposed frameworks allow us to implement operational rules and constraints into the system design. In this paper, time-varying queuing network models are developed to provide a framework for integrated departure and surface air traffic management at airports. Applying the proposed models, we demonstrate aircraft Departure Metering at a case study airport to reduce both airport surface congestion and departure queue at a runway threshold while utilizing maximum runway throughput. Finally, this paper discusses future extensions of the proposed model-based frameworks including their various applications for supporting collaborative decision-making and operations among stakeholders in air traffic management.**

***Keywords*—airport operation; departure management; surface management; queuing theory; system design**

I. Introduction

The performance of the air traffic systems depends on efficient operations at several levels: en route, arrival and departure, and ground operations. Although the development of traffic is subject to regular fluctuations (cf. [1]), the number of flights is also expected to increase in the future. However, the available airspace is limited and traffic demands must be balanced with available capacity. The requirements for efficient air traffic management are increasing and it is expected that the flights are not only carried out punctually and safely but also in ecological aspects justifiable and economically affordable. This extensive catalog of criteria limits the options for efficient management and requires a holistic, integrative approach [2, 3] in addition to the established optimization efforts in multi-objective trajectories [4–6], complex air space design [7, 8], airport ground and turnaround operations [9, 10], or airline/ network approaches [11, 12]. Accordingly, our study proposes a model-based framework, which enables time-varying control while balancing the air traffic flows. We focus on integrated airport departure and surface operations and propose a time-varying queuing model as part of a holistic framework.

Airport is a node in global aviation networks, thus airport operation highly influence on the behavior of air traffic flows. Increasing air traffic generates congestion, particularly at and around major airports [13], resulting in bottlenecks that propagate aircraft delay to entire air transport networks [14]. Reducing Runway Safety (RS)-related events and fuel consumption are major requirements for aircraft arrival, departure and surface air traffic operations. ICAO reported that RS-related events, such as ground collisions at the airport, led to the highest percentage of accidents involving destruction or substantial damage of aircraft [15]. Regarding fuel consumption, the authors found that aircraft departure queues on a single runway at Tokyo International Airport (RJTT) wasted more than one kiloton of fuel per year [16]. Designing efficient management concepts that integrate aircraft arrival, departure, and surface operations support not only Air Traffic Controllers (ATCos) but also airline and airport operators, and ground handlers. These concepts must provide efficient performances at stochastic features in air traffic, such as taxi-out times of departure aircraft, ground speed during taxiing, pushback duration, or arrival and departure times at runway thresholds.

In particular, a key operation for managing departure traffic is Departure Metering (DM), which allocates appropriate holds to departing aircraft at their gates. [17, 18]. The goal here is to reduce the departure queue at runway entry points while maintaining runway throughput. In a research study, the NASA ATD-2 project developed a DM logic, which is used to compute gate-hold time for each flight based on its predicted taxi-out time. The effectiveness of this approach has been demonstrated at Charlotte Douglas International Airport [19]. Badrinath et al. [20] developed queuing networks using a $D(t)/E_k(t)/1$ fluid queue, which models departure traffic from a single ramp to multiple departure runways and applied both optimal control and NASA ATD-2 logic to three major airports in the states. Taxi-out times from 60 to 70% of flights were estimated with an error margin of five minutes. The accuracy of these estimates, however, does not perform well

for the DM operation.

For further studies, a DM algorithm would be developed to mitigate airport surface congestion at the apron and taxi areas under the impact of arrival traffic. By coupling with the Departure Manager (DMAN), the Surface Manager (SMAN) is a management tool responsible for calculating appropriate gate release times and optimized taxi trajectories of departure aircraft with respect to planned takeoff times [21]. Integrated systems (coupled DMAN and SMAN) were developed to optimize time-based aircraft ground trajectories [22, 23]. In particular, Gerdes and Schaper [22] demonstrate that speed control (time-based trajectories) as a new feature for surface management could improve runway sequencing. Difficulties in optimizing time-based aircraft trajectories include handling operational uncertainties during actual airport operations. Moreover, conformance monitoring of time-based aircraft ground trajectories may increase ATCo's workload under current airport operations. Hasnain et al. [24] developed model-free and learning-based DM and surface hotspot prediction at Singapore Changi Airport. The simulation results showed a reduction in both surface congestion and departure queues, but departure-sequencing and delay-allocation rules were unknown in the model-free framework. It is also unclear how uncertainties in time-based ground trajectories impact the DM logic.

With the above background in mind, this paper proposes a model-based design integrating aircraft departure and surface traffic operation, which is resistant to uncertainties in aircraft trajectories while applying stochastic models. We aim to design highly interpretative airport systems for stakeholders participating in Airport Collaborative Decision-Making (ACDM) [18]. For this purpose, we develop a time-varying queuing network model, based on which we provide a framework integrating aircraft departure and surface operations. The proposed model-based framework enables the implementation of departure sequencing and delay allocation rules to motivate more cooperative taxi-out time operations among stakeholders in ACDM after target takeoff approval (TSAT).

This paper is organized as follows. Section II outlines the model-based framework for integrating aircraft departure and surface traffic operation. Section III develops the queuing network models using a $G(t)/GI/s(t)$ time-varying fluid queue, which enables to quantitatively estimate the aircraft departure-queue length and waiting time and surface traffic congestion according to the air traffic inflow and outflow rates. Applying the model-based framework, Section IV demonstrates the effectiveness of coupling departure and surface air traffic operation in day operation at RJTT airport. Section V discusses future extensions of the proposed model-based frameworks and their applications to design ATM systems for supporting collaborative actions among stakeholders. Finally, Section VI provides concluding remarks.

II. Design of the Model-based Framework

A. Overview of Integrated Departure and Surface Operations

The model-based framework is designed for integrating aircraft departure and surface traffic operation at an airport. Fig. 1 illustrates the proposed model-based framework, including DMAN, SMAN, and its integration. The output of the DMAN and SMAN coupling is TSAT, which gives taxi-out times to departure aircraft at terminal gates to mitigate surface traffic congestion and minimize the departure queue at the runway threshold while maximizing runway throughput.

In the proposed framework, DMAN is developed to calculate draft TSAT, which assigns gate holds to departure aircraft at terminal gates. DMAN outputs the draft TSAT to minimize the departure queue at the runway threshold while maximizing runway throughput. It must perform efficiently amid uncertain air traffic trajectories. Accordingly, the proposed DMAN first estimates departure rates at assigned time intervals. Secondly, it calculates the draft TSAT for allocating departure delay to control departure rates following rule-based sequencing and delay allocation. Accordingly, the proposed DMAN employs a "flow-based" design, which controls departure traffic rates at the terminal gates by draft TSAT. To control the departure rates, departure-queue length is estimated using queuing network models. To estimate the departure-queue length, Target Off Block Time (TOBT) lists and aircraft taxi-time predictions are input to DMAN.

SMAN takes the rules of 1) taxi-time prediction and 2) updating the draft TSAT to mitigate surface traffic congestion. One of the author's studies developed Machine Learning (ML) models for taxi-time prediction and confirmed that applying the ML prediction to DM reduced the departure queue [25, 26], due to more accurate taxi-time prediction. Accordingly, the proposed SMAN implements the ML-based taxi-time prediction model and the prediction is used in the DMAN to estimate the departure queue. SMAN also estimates the Traffic Volume (TV) at surface congestion bottlenecks at the airport. TV defines the total number of potential aircraft involved in potential bottleneck areas using queuing network models. Based on the estimation of time-varying TV, SMAN updates the draft TSAT to minimize the maximum peaks of TV and thereby mitigate surface congestion. Departure aircraft are selected to update TSAT following the sequencing and delay-allocation rules assigned.

B. Departure Management

The DMAN requires the following system inputs.

- TOBT lists (Callsign and TOBT sets)
- Predicted taxi time of the departure aircraft
- Estimated aircraft arrival time (shared by the Arrival Manager (AMAN))
- Statistic data of Runway Occupancy Time (ROT) and departure separation time at runway thresholds, which gives service time distribution to the departure queuing model
- Any information/data to execute departure-sequencing and delay-allocation rules

Using these inputs, DMAN functions are given as follows.

- Estimate departure-queue length and waiting time at the runway threshold (based on the departure queuing model and ML-based taxi-time prediction)

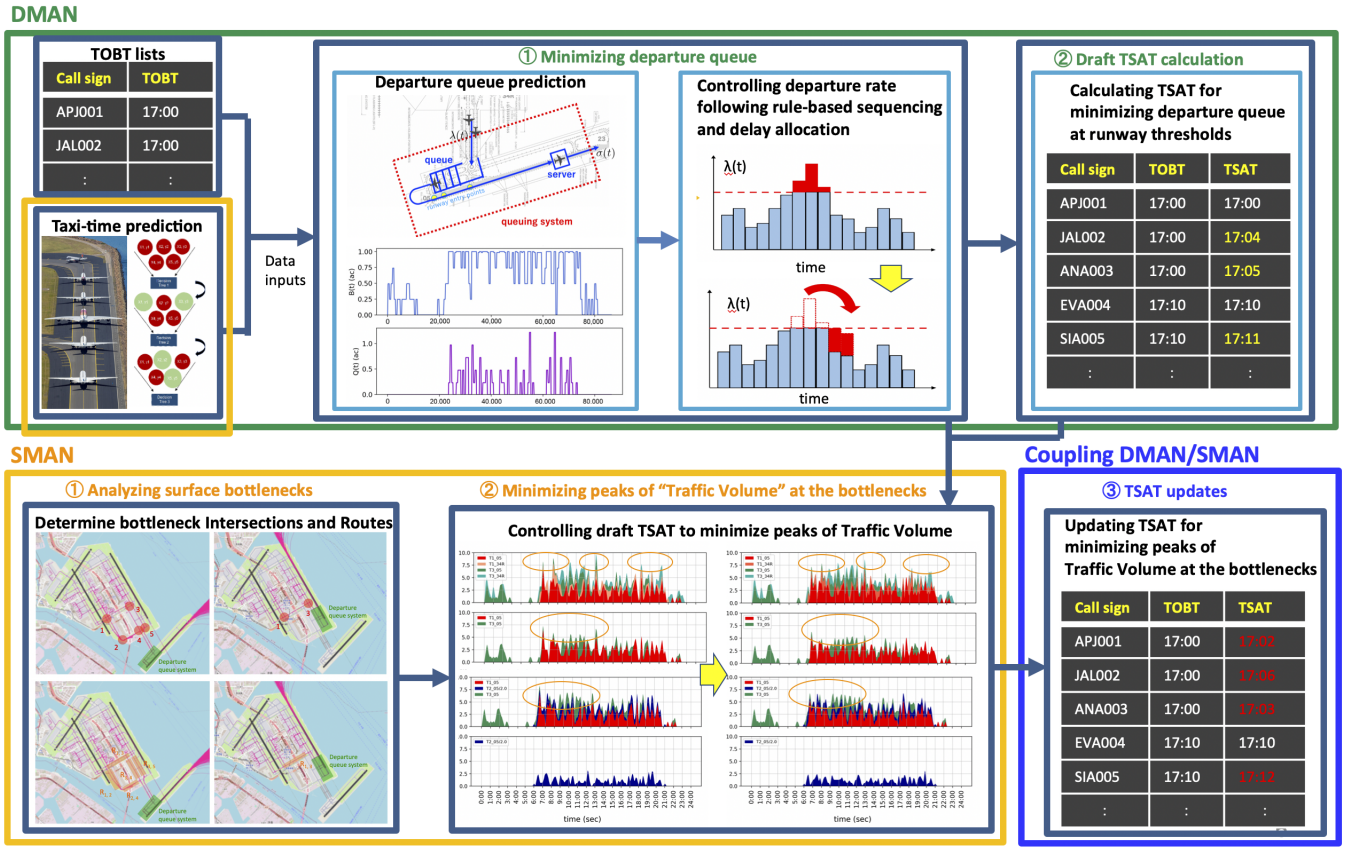

Figure 1: Integrated Departure and Surface Management in the Proposing Framework. DMAN calculates draft TSAT to minimize departure queue at runway thresholds (top). SMAN updates the draft TSAT to mitigate surface congestion (bottom, left). According to the coupling of DMAN and SMAN, TSAT is given to minimize both departure queue and surface traffic congestion (bottom, right).

- Calculate the ideal departure rate at the runways to minimize the departure queue while maximizing runway throughput
- Select target departure aircraft to be delayed following rule-based departure-sequencing and delay allocation
- Calculate draft TSAT for controlling the departure rate at the runway

The outputs of DMAN are draft TSAT, which minimizes departure queues at runway thresholds. In order to mitigate air traffic surface congestion by applying TSAT, SMAN updates the draft TSAT as follows:

C. *Surface Management*

The SMAN requires the following inputs.

- Draft TSAT lists (callsigns, original TOBT, draft TSAT)
- Departure gates and terminals information corresponding to the aircraft on the draft TSAT lists
- Bottleneck areas (intersections, routes, etc.) where SMAN estimates TV
- Statistic data of taxi-time, which is the service time distribution assigned to the surface-queuing model
- Any information/data to execute the departure sequencing and delay-allocation rules

These inputs are used to enable the SMAN functions, which are given as follows.

- Estimate TV according to the aircraft departure traffic flow (In our current model, departure traffic flows are grouped by departure terminal and runway combinations)
- Select target departure aircraft to reduce the TV peaks
- Updates departure-sequencing and allocates additional departure delay on the draft TSAT (Update draft TSAT)

Coupling of DMAN and SMAN outputs TSAT, which reduces both departure queue and surface air traffic congestion, as explained above.

Bottlenecks on the Airport Surface: To mitigate surface congestion, firstly bottlenecks on the surface operation are clarified at a target airport. In this paper, northerly wind operation at RJTT is selected as a case study airport operation.

RJTT is Japan's busiest airport, and the world's fourth busiest airport by passenger traffic [27]. As shown in Figure 2, the airport has four runways and three terminals. The four runways, a set of parallel north–south runways (34L/16R and 34R/16L) and two southwest–northeast crosswind runways (22/04 and 23/05), are used at RJTT. The use of the runways depends on wind direction. The northerly wind operation accounted for about 70% of the total, taking a larger share than the southerly wind operation. Figure 3 shows the runway usage of departures and arrivals at RJTT in the northerly wind operation. Aircraft arrive at either runway 34L or runway 34R, and departing aircraft takeoff from runway 05 or runway 34R,

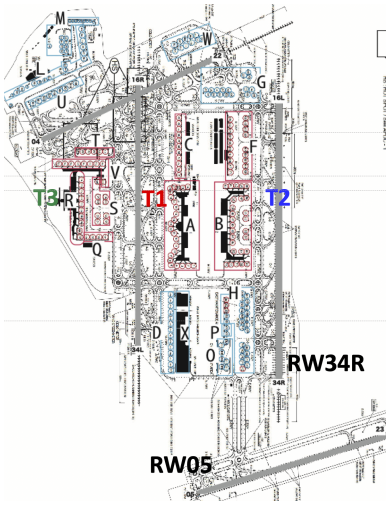

Figure 2: RJTT surface configuration

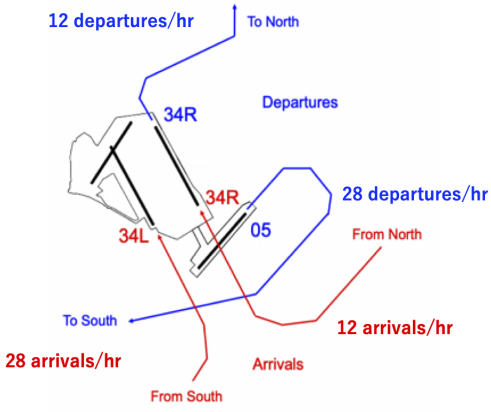

Figure 3: RJTT northerly wind operation.

depending on their origin/destination airports. Runway 05 is used only for departure operation, allowing a maximum of 28 departures in an hour. Runway 34R allows a maximum of 12 departures in an hour. In this study, we focus on the departure traffic at runway 05.

Two types of bottlenecks are defined according to the operational features at the case study airport (RJTT): Bottleneck Intersection Area (BIA) and Bottleneck Surface Route (BSR). BIAs define areas where the aircraft surface traffic intersects and BSRs define taxi routes connecting BIAs.

Figs. 4 and 5 show BIAs and BSRs with aircraft departure tracks between three terminals (T1, T2, T3) and departure runways (RW05 and RW34R). There are five BIAs and BSRs defined on the RJTT surface.

The five BIAs are defined by their attributes and inflow traffic rates (inflow rates) into each BIA as shown in Tab. I. If the inflow traffic is uniquely determined, which means the inflow traffic has no other choices of intersections except them in the BIA, the attribute is classified as independent. If the inflow traffic has alternative intersections in other BIAs, the attribute is classified as dependent; for example, inflow traffic into BIAs 4 and 5 have a choice to intersect both areas,

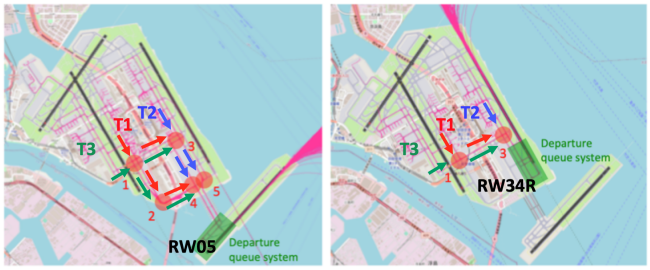

Figure 4: BIAs at RJTT. BIAs are shown in circles with departure traffic flows from each the terminal.

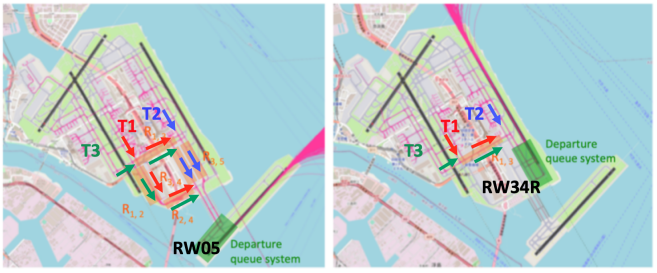

Figure 5: BSRs at RJTT. BSRs are shown in rectangles connecting BIAs with departure traffic flows from each the terminal.

whereupon their attribute is dependent.

Inflow rate λ_i varies over time and is defined using aircraft departure rates from terminals, T1, T2, T3, to departure runways, RW05 and RW34R, $\lambda_{T\in\{T1,T2,T3\},RW\in\{05,34R\}}$, as shown in Tab. I.

Concept of Traffic Volume: We define Traffic Volume (TV), B, as the total amount of potential aircraft intersecting BIAs and BSRs at time t. Applying the time-varying fluid queue model[28, 29], TV is quantitatively estimated as a time-varying function as shown in Section III. In this paper, TV at BIA, B_i, TV at BSR, $B_{j,k}$, are defined using the TV between the terminals and runways, $B_{T\in\{T1,T2,T3\},RW\in\{05,34R\}}$, as shown in Tabs. II and III. In Tab. III, BSRs are named as $R_{j,k}$ which connect the initial BIA j and the final BIA k. $n_{j,k}$ is the number of routes connecting BIA j and BIA k.

III. Modeling Aircraft Departure and Surface Traffic Flow via Queuing Networks

A. Queuing Network Models using $G(t)/GI/s(t)$ Time-Varying Fluid Queue

Now the queuing networks for aircraft departure and surface traffic at RJTT are modeled. Fig. 2 shows the corresponding gates and terminal configurations. All gates are grouped using letters A to X. Groups A and C belong to T1, B, and F

TABLE I. BIA definition

i	Attribute	Inflow rate, λ_i
1	Independent	$\lambda_1 \equiv \lambda_{T3,05} + \lambda_{T3,34R} + \lambda_{T1,05} + \lambda_{T1,34R}$
2	Independent	$\lambda_2 \equiv \lambda_{T3,05} + \lambda_{T1,05}$
3	Independent	$\lambda_3 \equiv \lambda_{T3,34R} + \lambda_{T1,34R} + \lambda_{T2,05} + \lambda_{T2,34R}$
4	Dependent	$\lambda_4 + \lambda_5 \equiv \lambda_{T1,05} + \lambda_{T2,05} + \lambda_{T3,05}$
5	Dependent	$\lambda_{T1,05} + \lambda_{T3,05} \leq \lambda_4 \leq \lambda_{T1,05} + \lambda_{T2,05} + \lambda_{T3,05}$, $0 \leq \lambda_5 \leq \lambda_{T2,05}$

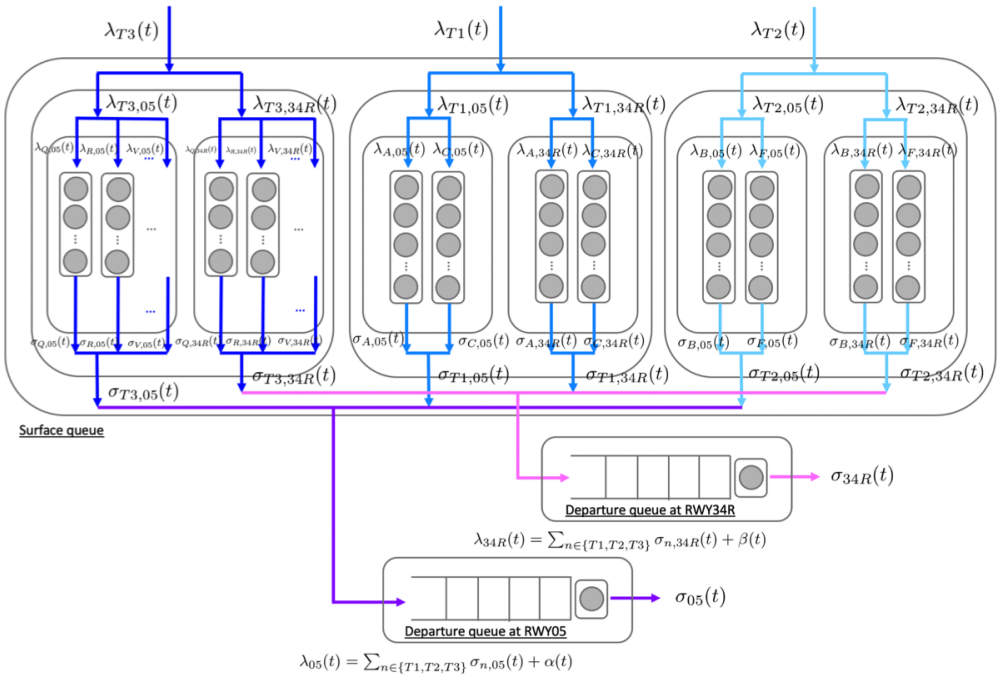

Figure 6: Airport Queuing Networks. In the model, one circle presents one aircraft. In the surface queue (top), time-varying aircraft numbers are counted according to the inflow rates (departure rates of each terminal gate) and service time (taxi time). The departure queue estimates aircraft waiting time at each runway threshold based on time-varying departure rate and service time at the departure runway (bottom).

TABLE II. TV definition at BIAs

i	Attribute	TV, B_i
1	Independent	$B_1 \equiv B_{T3,05} + B_{T3,34R} + B_{T1,05} + B_{T1,34R}$
2	Independent	$B_2 \equiv B_{T3,05} + B_{T1,05}$
3	Independent	$B_3 \equiv B_{T3,34R} + B_{T1,34R} + B_{T2,05} + B_{T2,34R}$
4	Dependent	$B_4 + B_5 \equiv B_{T1,05} + B_{T2,05} + B_{T3,05}$
5	Dependent	$B_{T1,05} + B_{T3,05} \le B_4 \le B_{T1,05} + B_{T2,05} + B_{T3,05}$, $0 \le B_5 \le B_{T2,05}$ $B_4 \approx B_{T1,05} + \frac{B_{T2,05}}{2} + B_{T3,05}$, $B_5 \approx \frac{B_{T2,05}}{2}$

TABLE III. TV definition at BSRs

$R_{j,k}$	Attribute	$n_{j,k}$	TV, $B_{j,k} \times n_{j,k}$
$R_{1,2}$	Independent	2	$B_{1,2} \times n_{1,2} \equiv B_{T3,05} + B_{T1,05}$
$R_{1,3}$	Independent	1	$B_{1,3} \times n_{1,3} \equiv B_{T3,34R} + B_{T1,34R}$
$R_{2,4}$	Independent	1	$B_{2,4} \times n_{2,4} \equiv B_{T3,05} + B_{T1,05}$
$R_{3,4}$	Dependent	1	$B_{3,4} \times n_{3,4} + B_{3,5} \times n_{3,5} \equiv B_{T2,05}$
$R_{3,5}$	Dependent	1 or 2 $\approx$ 1	$B_{3,4} \times n_{3,4} \approx B_{3,5} \times n_{3,5} \approx \frac{B_{T2,05}}{2}$

to T2, and Q, R, S, T, and V to T3 respectively. Most domestic flights use T1 and T2 and international flights use T3. Accordingly, the departure rates from gate groups at each terminal to the departure runways, $\lambda_{T\in\{T1,T2,T3\},R\in\{05,34R\}}(t)$, are shown as follows.

$$\lambda_{T1,R\in\{05,34R\}}(t) = \sum_{n_1\in\{A,C\}} \lambda_{n_1,R\in\{05,34R\}}(t) \quad (1)$$

$$\lambda_{T2,R\in\{05,34R\}}(t) = \sum_{n_2\in\{B,F\}} \lambda_{n_2,R\in\{05,34R\}}(t) \quad (2)$$

$$\lambda_{T3,R\in\{05,34R\}}(t) = \sum_{n_3\in\{Q,R,S,T,V\}} \lambda_{n_3,R\in\{05,34R\}}(t) \quad (3)$$

$\lambda_{T\in\{T1,T2,T3\},R\in\{05,34R\}}(t)$ in (1), (2), (3) are inflow rates to the surface-queuing network models. Outflow rates from the surface-queuing network models, $\sigma_{T\in\{T1,T2,T3\},R\in\{05,34R\}}(t)$, are given as follows.

$$\sigma_{T1,R\in\{05,34R\}}(t) = \sum_{n_1\in\{A,C\}} \sigma_{n_1,R\in\{05,34R\}}(t) \quad (4)$$

$$\sigma_{T2,R\in\{05,34R\}}(t) = \sum_{n_2\in\{B,F\}} \sigma_{n_2,R\in\{05,34R\}}(t) \quad (5)$$

$$\sigma_{T3,R\in\{05,34R\}}(t) = \sum_{n_3\in\{Q,R,S,T,V\}} \sigma_{n_3,R\in\{05,34R\}}(t) \quad (6)$$

Outflow rates $\sigma_{T\in\{T1,T2,T3\},R\in\{05,34R\}}(t)$ in (4), (5), (6) are inflow rates $\lambda_{R\in\{05,34R\}}(t)$ to the departure-queue models (7). $\beta_{R\in\{05,34R\}}(t)$ are inflow rates to departure runways except from the three terminals.

$$\lambda_{R\in\{05,34R\}} = \sum_{n\in\{T1,T2,T3\}} \sigma_{n,R\in\{05,34R\}} + \beta_{R\in\{05,34R\}} \quad (7)$$

Fig. 6 presents aircraft surface and departure queuing network models using inflow and outflow rates in (1) to (7).

B. Aircraft Departure Queue Models

Aircraft departure-queue models, which estimate time-varying departure-queue length and waiting time at runway thresholds, were designed using a $G(t)/GI/s(t)$ time-varying fluid queue [16, 30]. Fig. 7 illustrates the departure-queue model at RW05 of RJTT. In the model, the inter-arrival

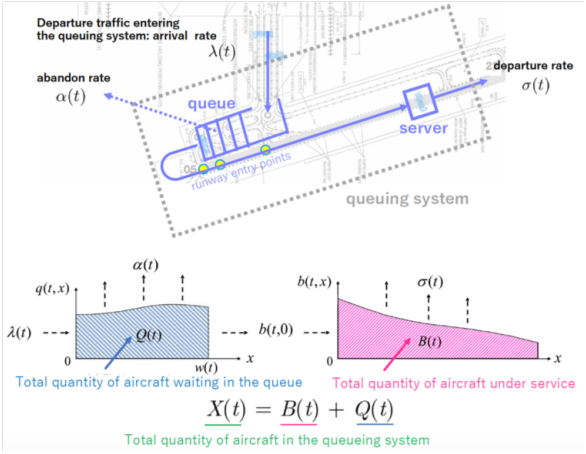

Figure 7: Aircraft departure queue model. The top figure explains the departure queuing system using time-varying arrival rate (inflow rate into the queuing system), abandon rate (aircraft rate leaving the queuing system before taking the service), and departure rate from the runway. The bottom figure explains that the total amount of departure aircraft in the queuing system, $X(t)$, is the sum of the departure aircraft in the queue $Q(t)$, and the departure aircraft under service $B(t)$ (using the runway).

time, which determines the inflow rate (departure traffic rate entering the queuing system), is the time between two consecutive departure aircraft entering the queuing system at a distance of 0.5 NM from the runway entry points. Service time is defined as the sum of the Runway Occupancy Time (ROT) and spacing time between the proceeding aircraft at the runway entry point. Server is given as the number of departure aircraft allowed to occupy the runway. The number of servers varies over time and is always less than 1.0. The total quantity of aircraft in the queuing system at time t, $X(t)$, is given as a sum of the total quantity of aircraft under service $B(t)$, and the total quantity of aircraft waiting in the queue $Q(t)$. Algorithms are summarized in [16].

C. Aircraft Surface Queue Models

In the aircraft surface queuing networks, we estimate TV using the $G(t)/GI/s(t)$ time-varying fluid queue. Here we describe TV corresponding to each surface-queuing model in Fig. 6 as $B(t)$, corresponding inflow rate (departure rate from each group of gates) as $\lambda(t)$ and corresponding outflow rate as $\sigma(t)$.

The total number of departure aircraft in time interval $[0, t]$, $\Lambda(t)$, is given as follows when $t \geq 0$.

$$\Lambda(t) \equiv \int_0^t \lambda(u)du \tag{8}$$

Using the cumulative distribution function (CDF) and probability density function (PDF) of taxi-time, $G(x)$ and $g(x)$, $\bar{G}(x)$ and $h_G(x)$ are defined as follows.

$$\bar{G}(x) \equiv 1 - G(x) \tag{9}$$

$$h_G(x) \equiv \frac{g(x)}{\bar{G}(x)} \tag{10}$$

Here $B(t)$ is given using (8), (9), (10) as follows.

$$\begin{aligned} B(t) &= \int_0^t \bar{G}(x)\lambda(t-x)dx + \int_0^\infty \frac{\bar{G}(x+t)}{\bar{G}(x)} b(0,x)dx \\ &\leq \Lambda(t) + B(0) \end{aligned} \tag{11}$$

$\sigma(t)$ is given using (10) as follows.

$$\sigma(t) \equiv \int_0^\infty b(t,x)h_G(x)dx \tag{12}$$

$b(t,x)$ in (12) is given as follows.

$$b(t,x) = \begin{cases} \bar{G}(x)\lambda(t-x), & x \leq t \\ \frac{\bar{G}(x)}{\bar{G}(x-t)} b(0,x-t), & x > t \end{cases} \tag{13}$$

The surface queue models assume all aircraft are under service, so $X(t) = B(t)$ in the model.

Combining the departure-queue and surface queue models in Sections III-B and III-C, an airport-queuing network model was developed at RJTT. This model was then implemented into the proposed framework of integrated DMAN and SMAN. The next section shows case study results applying the proposed framework into daily operation at RJTT.

IV. Case Study at Tokyo International Airport

This section presents how the designed framework (see Fig. 1) is applied to the case study airport. Section IV-A explains how DMAN calculates draft TSAT applying the departure queue model. Section IV-B describes how SMAN updates and draft TSAT are applied to the surface queue models, and generate a TSAT, which mitigates both departure queue at the runway threshold and surface air traffic congestion.

A. Calculating Draft TSAT Minimizing the Departure Queue

Predicting aircraft departure queue: In the proposed framework shown in Fig. 1, firstly DMAN predicts the departure queue based on the departure-queue model, taxi-time prediction model, TOBT lists, and statistical data. In this case study, prediction errors involving taxi time are not considered for simplicity since the purpose of this section is to demonstrate a framework applying the queuing network models. Instead of TOBT, this case study uses Actual Off Block Time (AOBT) recorded in daily operations.

In this case study, the maximum number of servers, $s_{max}(t)$, is given to identify the ideal $\lambda(t)$, which is the inflow rate minimizing the departure queue. When $s_{max}(t) > 1.0$, it allows a departure queue at the runway threshold, however, it prevents runway slot losses under uncertainties in airport operation. Fig. 8 show the prediction results $X(t)$ and $\lambda(t)$ and compare ideal $\lambda(t)$, which realize $X(t) < s_{max}$ where $s_{max} = 1.0, 1.25, 1.5$, at ten-minute time intervals. If the system allows larger s_{max}, it also allows larger $\lambda(t)$ for excluding the departure queue.

Delay allocation rules

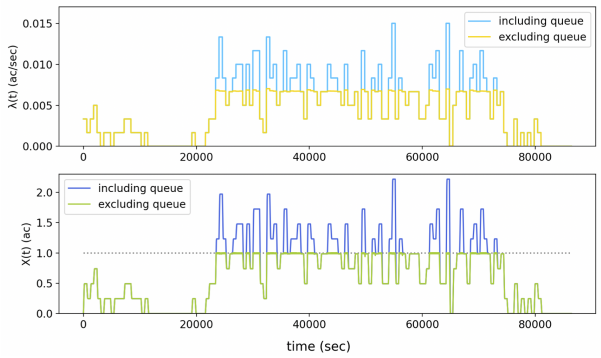

(a) $s_{max} = 1.0$

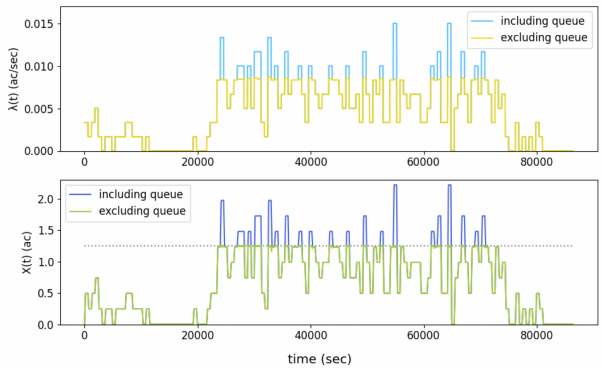

(b) $s_{max} = 1.25$

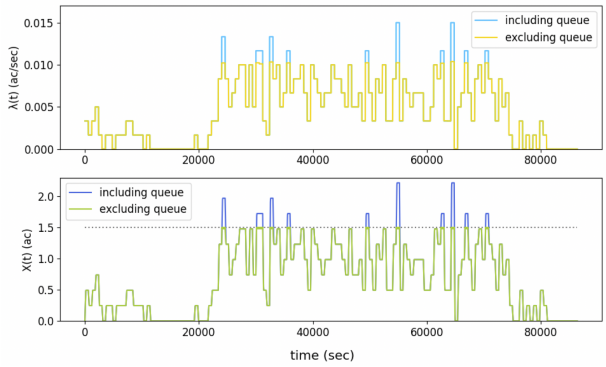

(c) $s_{max} = 1.5$

Figure 8: Comparison of ideal $\lambda(t)$ where $X(t) < s_{max}$. These figures shows that the value of s_{max} controls allowable departure queue length at the runway threshold. When s_{max} grows, the departure queue model allows longer departure queue length.

Controlling aircraft inflow rate: Based on the prediction above, the inflow rate $\lambda(t)$ is controlled to satisfy $X(t) < s_{max}$ at RW05. Here $s_{max} = 1.25$ is given to allow five departure aircraft to enter the departure-queue system every ten minutes. Regarding the RJTT RW05 operation, this assumes a realistic departure queue since the maximum number of runway departures is 28 per hour. Fig. 9 compares the original inflow rate, $\lambda_{org}(t)$ where $X(t) \geq s_{max}$, and the updated inflow rate, $\lambda_{upd}(t)$ which is controlled to satisfy $X(t) < s_{max}$, into the departure-queue system. In this way, it realizes "Runway Flow Control" which controls departure air traffic at assigned time intervals.

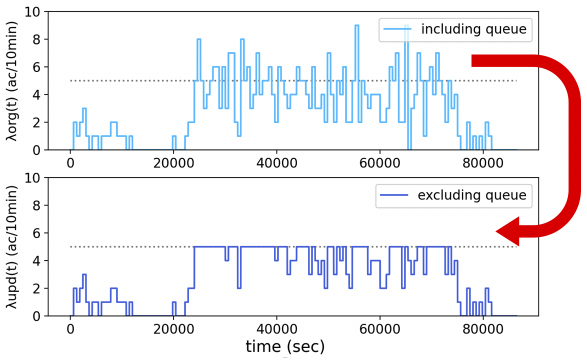

Figure 9: Controlling $\lambda(t)$ to satisfy $X(t) < s_{max}$. Draft TSAT generates taxi-out times for keeping departure queue length below s_{max}.

Rule-based departure-sequencing and delay allocation: To control the inflow rate to realize λ_{upd}, we need to select departure aircraft to delay the taxi-out time at the terminal gates. Departure-sequencing and delay-allocation rules are given as follows:

Departure-sequencing rules

- The best departure-sequencing rule will be investigated considering multiple criteria, such as operational fairness, minimizing fuel consumption (e.g., selecting the target aircraft depending on the aircraft types), or minimizing total departure delays.
- This case study employs the First-Come First-Served (FCFS) rule, which decides departure sequences following the predicted departure sequencing at 0.5 NM before the runway entry points at RJTT RW05. At ten-minute intervals, departure aircraft entering the system later than the fifth-earliest aircraft are delayed to the next-latest time interval respectively.
- In conjunction with the departure sequencing rules, departure delay allocation rules are determined.
- This case study employs delay-allocation rules following the FCFS-based departure-sequencing as explained in Fig. 10. In the example, the sixth aircraft in the ith time-interval is delayed and becomes the first aircraft at the $i+1$th time interval. Subsequently, the second aircraft at the $i+1$th time interval is delayed to maintain a two-minute interval between the first aircraft. Following this rule, departure delays are allocated to all aircraft in the one-day operation departing from RJTT RW05.

Fig. 11 shows the average delay of departures at all time intervals according to controlling $\lambda_{org}(t)$ to $\lambda_{upd}(t)$.

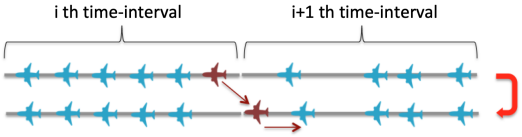

Figure 10: Delay allocation rules. In this example, the 6 th aircraft in the i th time-interval is delayed in the $i+1$ th time-interval to keep the maximum departures below 5 aircraft in each time-interval.

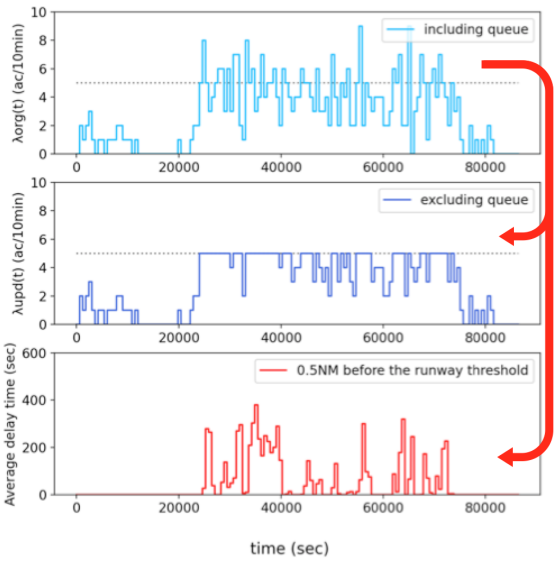

Figure 11: Average departure delay time at terminal gates according to draft TSAT. Draft TSAT works to control departure rates at the runway threshold (top: original, middle: controlled by draft TSAT), then shift waiting time at the runway threshold to gate-hold time at each terminal (below).

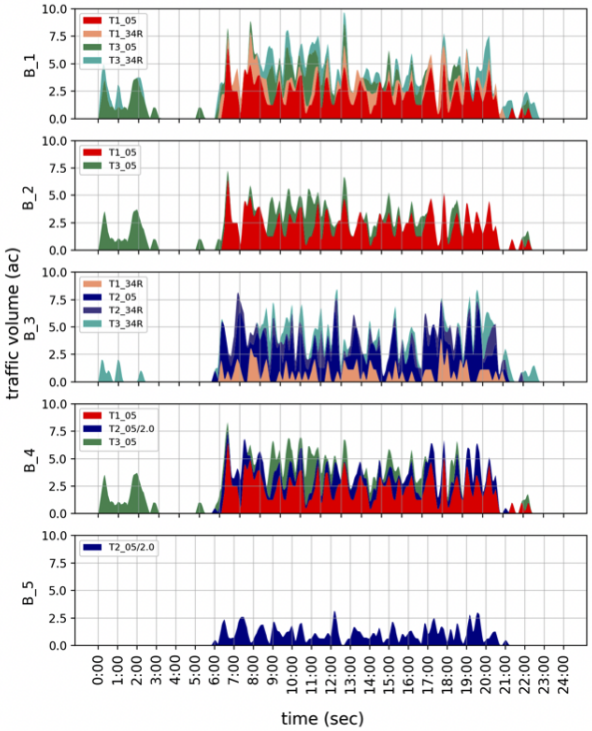

Figure 12: Estimating TV at BIAs. The surface queue models are applied to estimate TV. TV is described according to each set of departure terminals to runways.

Calculating draft TSAT: Based on the departure-sequencing and delay-allocation rules, the draft TSAT is given by adding the original TOBT to the required departure delay at the runway threshold. Tab. IV shows the total and maximum departure delays and the number of delayed departure aircraft per day. In total, the draft TSAT reduced departure waiting time at the runway threshold by 6914.6 seconds by delaying the departures at the terminal gates. The maximum hold at the terminal gates was 380.0 seconds, which means all delayed departure aircraft were allocated to time intervals next to their original slots. A total of 58 departure aircraft, 14% of daily departures, were delayed at the terminal gates during the daily operation.

TABLE IV. Effectiveness of the draft TSAT

Total delay time	**Max. delay time**	**Total number of delayed aircraft**
6914.6 (sec)	380.0 (sec)	58 (ac) in a day (Total 409 departures in a day)

B. Updating TSAT Mitigating Surface Congestion

Estimating TV peaks: Assuming all departures follow the draft TSAT when they taxi out from the terminal gates, the proposing SMAN estimates aircraft surface traffic congestion at BIAs and BSRs applying the surface queue models. Figs. 12 and 13 show the estimated TV at BIAs and BSRs during daily operation and depending on surface traffic from terminals to departure runways. As shown in Figs. 12 and 13, TV peaks emerge, which dramatically increase the values. This case study identified that the surface traffic contributing to the TV peaks could be divided into three groups: ”T1_RW05”, ”T2_RW05”, and ”T3_RW05”, which taxi out terminal T1, T2, and T3, to RW05, respectively.

Minimize TV peaks by additional departure delay allocation:

Based on the TV estimation, the SMAN allocates additional departure delays at terminal gates to minimize the TV peaks. To select the target departure aircraft subject to additional delay, two values are determined; the threshold of TV peaks and the maximum number of departure aircraft to delay at each time interval. If the maximum TV values at time intervals exceed the threshold value, the SMAN reduces the departure traffic contributing to the TV peaks. However, care should be taken to avoid losing runway departure slots. With balance in mind, this case study cites seven aircraft as the TV threshold and allows a maximum of two departing aircraft to be delayed from one time interval to the subsequent time slot. We then decide on departure-resequencing and delay re-allocation rules as follows

Departure re-sequencing rules

- Selecting departure aircraft to mitigate surface congestion (reduce TV peaks) may change departure-sequencing in DMAN in Section IV-A.
- According to the surface traffic features, this case study selects departure aircraft in ”T1_RW05” and ”T3_RW05” to reduce TV at BIA $i = 1$ (B_1), and ”T2_RW05” to reduce TV at BIA $i = 1$ (B_3) where TV > 7.
- This case study employed the FCFS rule following departure-sequencing at the parking gates at each terminal. The latest two aircraft for each time interval are delayed by a maximum of up to the subsequent time slot.

Delay re-allocation rules

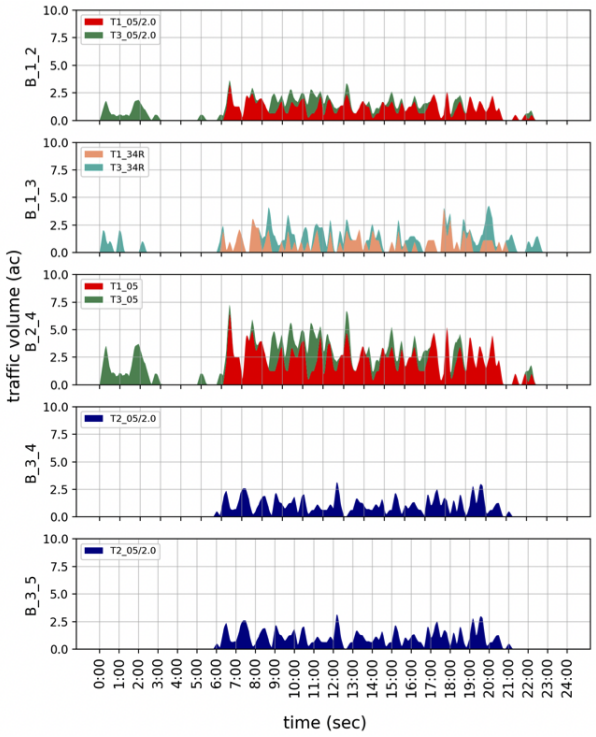

Figure 13: Estimating TV at BSRs. The surface queue models are applied to estimate TV. TV is described according to each set of departure terminals to runways.

- This case study employed the same rule in Section IV-A as shown in Fig. 10 for the delay re-allocation following the FCFS-based departure re-sequencing above.

Updating draft TSAT: Following the departure-resequencing and delay-allocation rules above, the draft TSAT was updated in the SMAN. Fig. 14 compares TVs at BIAs when the departures taxi out following the draft and updated TSAT. Most of the TV peaks were reduced by updating TSAT, however two TV peaks at B 3 increased because of departure traffic to RW34R. Although this case study controlled the TSAT of departures at RW05, the results indicated the need for TSAT control plus departures from RW34R to reduce all TV peaks.

Fig. 15 compares the original, DMAN (draft TSAT) controlled and DMAN and SMAN (updated TSAT) controlled inflow rate into the departure-queue system. By coupling DMAN and SMAN, the inflow rate is controlled by a maximum of two aircraft for each time interval.

Tab. V compares the DM effects. When the TSAT was updated by coupling DMAN and SMAN to reduce both departure queue and surface traffic congestion, the gate-hold times of the departure traffic increased to a total of 17127 seconds and a maximum of 1044 seconds because the DMAN/SMAN coupling allowed departure delays involving two time intervals. The total number of delayed aircraft increased to 74 per day. This case study indicated the need for a trade-off between minimizing departure delay and surface traffic congestion at RJTT.

TABLE V. Effectiveness of the draft and updated TSAT

DM	Total delay time	Max. delay time	Total number of delayed aircraft
DMAN	6914.6 (sec)	380.0 (sec)	58 (ac) in a day
Coupling DMAN/SMAN	17127 (sec)	1044 (sec)	74 (ac) in a day

V. Discussion

There are two main ways to streamline airport operations, which namely involve minimizing both departure queue and surface congestion. One is targeting airport design, including runways, terminals, terminal gates and taxiways and terminal gate configurations. The other is controlling air traffic time schedules, including dynamic terminal gate allocations and TSAT operations. There is a need to determine the best solution by combining both approaches under constraints at the target airports. The proposed queuing network models provide a rule-based framework to the design airport and its dynamic operation by balancing air traffic inflow and outflow rates while ensuring appropriate demand and capacity.

When these models were applied, the results of daily operation indicated a trade-off between departure delay and surface traffic congestion under the FCFS-based DM, which allowed departure-only delay from TOBT, while maintaining maximum throughput at the departure runway. To minimize both departure delay and surface congestion, one of the potential ways would be to allow TSAT earlier than TOBT. Furthermore, if EOBT could be distributed by minimizing TV in advance, this would also help reduce departure delay and surface congestion. Designing DM rules is important to motivate fair operations. For example, airlines which cooperate with ACDM, by providing TOBT into the ACDM system, would be able to achieve an ideal taxi-out time following TSAT. Accordingly, "contribution-based" airport operations will be discussed in future works. These DM rules will be evaluated amid uncertainties in aircraft trajectory prediction while applying ML models.

On the ATCo interaction, one potential shows the TV values to ground controllers. If the estimated TV values are high, this gives gate-hold options for the suggested departure aircraft based on sequencing and delay-allocation rules. Our future works will also involve designing man-machine interactions.

This study will also develop queuing network models and apply a framework for designing mobility systems in the future. On the airport-queuing networks, surface queue models will be advanced for TV estimation. On the further extensions of the framework, there are various applications of time-varying fluid queue networks in the context of controlling inflow and outflow traffic while taking capacity-demand balancing, e.g. air traffic flow management, airspace operations, airline networks, UTM/UAM operations (controlling cooperative airspace, vertiport networks), passenger/cargo traffic arriving/departing at/from airports into consideration. This study aims to design future mobility systems applying model-based frameworks.

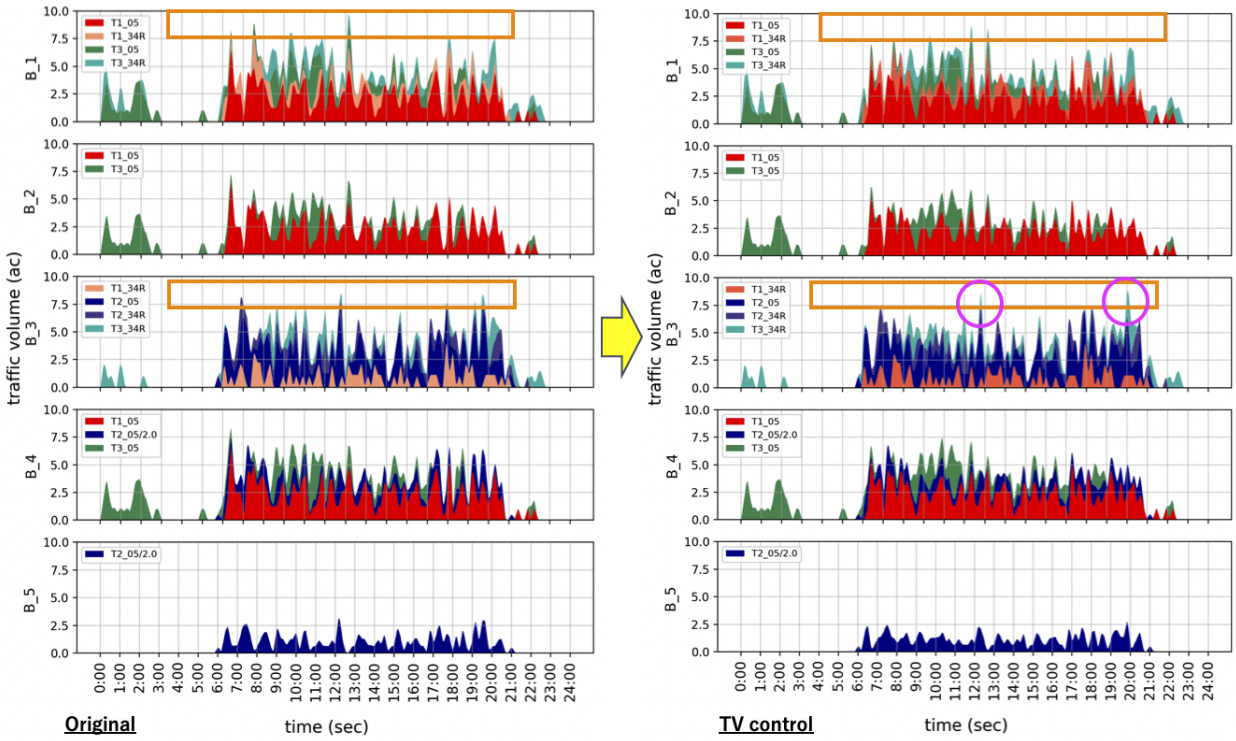

Figure 14: Implementation of traffic volume control. TSAT reduced most of TV peaks (see the areas in rectangles). However, some peaks increased as emphasized by circles on the right side. This indicates that the TV controls of RW05 departures should be integrated with these of RW34R.

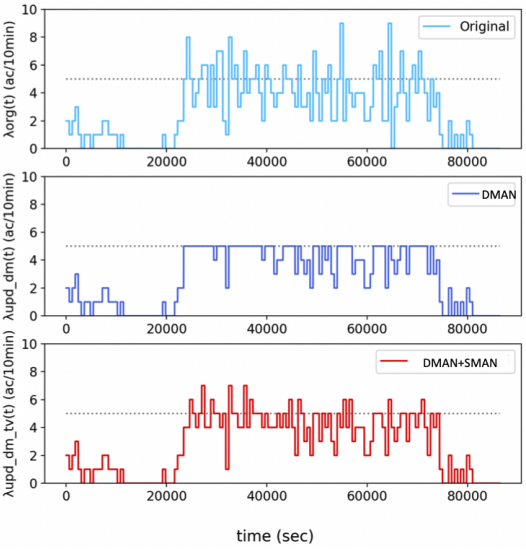

Figure 15: Comparing inflow rates into departure queue system (top: original, middle: controlled by draft TSAT, below: controlled by TSAT). TSAT controlled the departure rate while avoiding departure slot losses at the departure runway.

VI. Conclusion

This paper proposed a model-based framework for integrating aircraft departure and surface traffic operation using time-varying fluid queuing networks. An integrated DMAN/SMAN system was designed applying the framework and DM rules were implemented into the system to generate TSAT. By coupling DMAN and SMAN, TSAT successfully reduced both departure-queue and surface congestion while maintaining the assigned runway throughput during daily operation at RJTT. The simulation results clarified scope for a trade-off between departure hold (delay) time and surface congestion; departure delay increased by mitigating surface congestion. We discussed future works to design even better airport operation and scope for a future extension of the model-based framework was suggested in the discussion section.

Acknowledgment

This research was conducted under the CARATS initiative supported by the Civil Aviation Bureau (JCAB) of the Japanese Ministry of Land, Infrastructure, Transport, and Tourism. The authors are grateful to JCAB for providing air traffic data.

References

[1] IATA, "COVID-19 outlook for air travel in the next 5 years," 2020.

[2] T. Kistan *et al.*, "An evolutionary outlook of air traffic flow management techniques," *Progress in Aerospace Sciences*, vol. 88, pp. 15–42, 2017.

[3] J. Rosenow and M. Schultz, "Coupling of turnaround and trajectory optimization based on delay cost," in *2018 Winter Simulation Conference (WSC)*, 2018, pp. 2273–2284.

[4] A. Gardi, R. Sabatini, and S. Ramasamy, "Multi-objective optimisation of aircraft flight trajectories in the atm and avionics context," *Progress in Aerospace Sciences*, vol. 83, pp. 1–36, 2016.

[5] M. Zhang, A. Filippone, and N. Bojdo, "Multi-objective optimisation of aircraft departure trajectories," *Aerospace Science and Technology*, vol. 79, pp. 37–47, 2018.

[6] J. Rosenow, H. Fricke, and M. Schultz, "Air traffic simulation with 4d multi-criteria optimized trajectories," in *2017 Winter Simulation Conference (WSC)*, 2017, pp. 2589–2600.

[7] M. Sergeeva *et al.*, "Dynamic airspace configuration by genetic algorithm," *Journal of Traffic and Transportation Engineering*, vol. 4, no. 3, pp. 300–314, 2017.

[8] I. Gerdes, A. Temme, and M. Schultz, "Dynamic airspace sectorisation for flight-centric operations," *Transportation Research Part C: Emerging Technologies*, vol. 95, pp. 460–480, 2018.

[9] I. Simaiakis and H. Balakrishnan, "A queuing model of the airport departure process," *Transportation Science*, vol. 50, no. 1, pp. 94–109, 2016.

[10] M. Schultz *et al.*, "Future aircraft turnaround operations considering post-pandemic requirements," *Journal of Air Transport Management*, vol. 89, p. 101886, 2020.

[11] J. Evler *et al.*, "Integration of turnaround and aircraft recovery to mitigate delay propagation in airline networks," *Computers and Operations Research*, vol. 138, p. 105602, 2022.

[12] E. Asadi, M. Schultz, and H. Fricke, "Optimal schedule recovery for the aircraft gate assignment with constrained resources," *Computers and Industrial Engineering*, vol. 162, p. 107682, 2021.

[13] L. Zhi Jun *et al.*, "Towards a greener extended-arrival manager in air traffic control: A heuristic approach for dynamic speed control using machine-learned delay prediction model," *Journal of Air Transport Management*, vol. 103, p. 102250, 2022.

[14] D. Lubig *et al.*, "Propagation of airport capacity improvements to the air transport network," in *2021 IEEE/AIAA 40th Digital Avionics Systems Conference (DASC)*, 2021, pp. 1–10.

[15] ICAO, "Safety reports," 2019. [Online]. Available: https://www.icao.int/safety/Pages/Safety-Report.aspx

[16] E. Itoh, M. Mitici, and M. Schultz, "Modeling aircraft departure at a runway using a time-varying fluid queue," *Aerospace*, vol. 9, no. 3, 2022.

[17] FAA Surface CDM Team, "US Airport Surface Collaborative Decision Making (CDM) Concept of Operations (ConOps) in the Near-Term: Applications of Surface CDM at United States Airports," 2012.

[18] EUROCONTROL Airport CDM Team, "Airport CDM Implementation-The Manual," 2018.

[19] S. Verma *et al.*, "Tactical surface metering procedures and information needs for charlotte douglas international airport," in *Advances in Human Aspects of Transportation*, N. Stanton, Ed. Cham: Springer International Publishing, 2019, pp. 157–169.

[20] S. Badrinath *et al.*, "Impact of off-block time uncertainty on the control of airport surface operations," *Transportation Science*, vol. 54, no. 4, pp. 920–943, 2020.

[21] E. Tuinstra and K. Haschke, "Generic Operational Concept for Pre-departure Runway Sequence Planning and Accurate Take-Off Performance Enabled by DMAN Interaction with Airport CDM and A-SMGCS Concepts," 2009.

[22] I. Gerdes and M. Schaper, "Management of time based taxi trajectories coupling departure and surface management systems," in *The 11th USA/Europe ATM R&D Seminar*, 2015.

[23] L. Nohren *et al.*, "Real-time calculation and adaptation of conflict-free aircraft ground trajectories," in *International Council of the Aeronautical Sciences Congress*, 2022.

[24] H. Ali *et al.*, "Dynamic hot spot prediction by learning spatial-temporal utilization of taxiway intersections," in *2020 International Conference on Artificial Intelligence and Data Analytics for Air Transportation (AIDA-AT)*, 2020, pp. 1–10.

[25] F. Kato and E. Itoh, "Applying machine learning to taxi-time prediction at tokyo international airport," in *International Council of the Aeronautical Sciences Congress*, 2022.

[26] ——, "Aircraft taxi-time prediction using machine learning and its application for departure metering," *(under review)*, 2023.

[27] Airports Council International (ACI), "Passenger traffic 2017 final (annual)," *Passenger Summary*, 2019.

[28] Y. Liu and W. Whitt, "The $g_t/gi/s_t + gi$ many-server fluid queue," *Queueing Systems*, vol. 71, pp. 405–444, 2012.

[29] W. Whitt, "Time-varying queues," *Queueing models and service management*, vol. 1, no. 2, 2018.

[30] E. Itoh, D. Iwata, and M. Schultz, "Developing a departure queue model towards integrated arrival and departure runway operation," in *International Council of the Aeronautical Sciences Congress*, 2022.